

SIMULATIONS OF THE NEUTRALIZING CAPACITY OF SILICATE ROCKS IN ACID MINE DRAINAGE ENVIRONMENTS¹

L. Edmond Eary,² and Mark A. Williamson

Abstract. Pyritic rocks with little or no carbonate mineral content generally produce acid mine drainage when exposed to the atmosphere and moisture. In the absence of carbonate minerals, it is often suggested that silicate minerals can provide some level of acid buffering. At the current time, databases of reaction kinetics are sufficiently detailed to allow calculations of the rates of silicate mineral dissolution reactions relative to the rate of pyrite oxidation. These types of calculations have been conducted for conditions of abiotic oxidation of pyrite by O₂ to estimate the acid neutralizing capacity of silicate rock types in terms of specific mineral contents. Using the criteria of maintaining a pH > 5.0 for 10-years, these calculations yield the following results for some generalized igneous rock types.

Rock Type	NP Range (kg CaCO ₃ /t)
Granite	0.6
Quartz	
Monzonite	2.0-2.7
Monzonite	2.2-3.0
Granodiorite	1.8-2.2
Quartz	
Diorite	18.9-29.2
Diorite	26.7-40.2
Gabbro	29.2-50.1

The results show that it is feasible to use geochemical model calculations to estimate neutralization potentials through reaction rate calculations, although these calculations tend to overestimate neutralization potentials of mafic rock types compared to experimental data. The rate calculations also point out the importance of the mafic mineral content for neutralizing acidity in that minerals, such as calcic plagioclase, forsterite, augite, and hornblende, may react rapidly enough to keep up with the rate of acid generation by pyrite oxidation under the right circumstances, whereas the felsic minerals, such as K-feldspar and albite, react too slowly to mitigate acid generation. The calculations also show the importance of secondary mineral formation in estimating neutralization potential in that equilibrium with goethite and gibbsite yields the low end of the range listed in the above table relative to equilibrium with amorphous Fe and Al hydroxides. Overall, the kinetics simulation procedures provide an efficient and inexpensive means to conduct scoping studies of likely pH conditions for carbonate-poor rocks that can be used to optimize sample selection for more detailed experimental testing or prediction of potential impacts from acid mine drainage based on petrological and mineralogical data in the absence of detailed experimental data.

¹ Paper presented at the 7th International Conference on Acid Rock Drainage (ICARD), March 26-30, 2006, St. Louis MO. R.I. Barnhisel (ed.) Published by the American Society of Mining and Reclamation (ASMR), 3134 Montavesta Road, Lexington, KY 40502

² L. Edmond Eary, Senior Geochemist and Mark A. Williamson, Senior Geochemist, Applied & Environmental Geochemistry Group, MFG Inc., 3801 Automation Way, Suite 100, Fort Collins, Colorado 80525

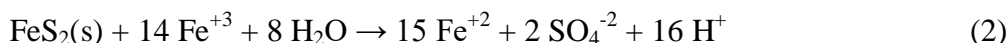
7th International Conference on Acid Rock Drainage, 2006 pp 564-577

DOI: 10.21000/JASMR06020564

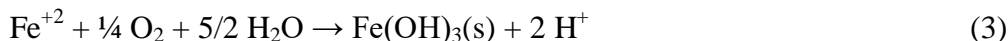
<https://doi.org/10.21000/JASMR06020564>

Introduction

Acid rock drainage is primarily the result of the oxidative dissolution of pyrite through reactions such as:



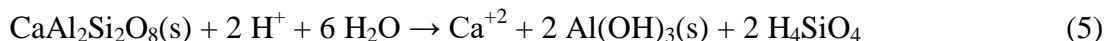
Under near-neutral pH conditions, the Fe^{+2} is oxidized and precipitated as hydroxide solids producing more acid as in:



It is generally recognized that dissolution reactions involving both carbonate and silicate minerals have the potential to neutralize the acid generated by sulfide oxidation through reactions such as:



and



In most rock-water systems, it is the carbonate minerals that, when present in sufficient quantities, provide the primary neutralizing capacity because they react rapidly enough to keep up with the rate of acid production from sulfide oxidation. In comparison, most silicate minerals are generally thought to not dissolve fast enough to preclude acid generation under most circumstances. Otherwise, acid rock drainage would not be the common phenomena that it is given the predominance of silicate rock types over carbonates in most mineralized districts. These concepts are generally well established and well described in many publications, including (e.g., ICARD, 2000; MEND, 1997; Nordstrom and Alpers, 1999; White et al., 1999).

Empirical observations of weathered rocks indicate that relative rates of silicate mineral dissolution increase with increasing thermodynamic instability under normal surficial conditions (Goldich, 1938). Experimental studies confirm the empirical observations and clearly show that high temperature minerals such as anorthite dissolve much more rapidly than feldspars (Fig. 1). As a result, mafic rocks comprised of minerals such as plagioclase, pyroxenes, olivines, and amphiboles generally provide for more acid neutralization potential than silicic rocks comprised of alkali feldspars, quartz, and micaceous minerals. A complication to this generalization is that mafic minerals generally contain more ferrous iron than silicic minerals. Under neutral to basic pH conditions, the ferrous iron dissolved from mafic minerals will be rapidly oxidized to ferric iron (Millero, 1985; Moses and Herman, 1989) and precipitated as ferric oxyhydroxides (Bigham et al., 1996; Langmuir and Whittemore, 1971). However, if the rock-water system eventually becomes acidic, then the iron dissolved from the mafic minerals could promote sulfide oxidation.

If one considered only relative reaction rates, then it might be expected that silicate mineral dissolution could have the capacity to prevent or at least limit acid generation under some circumstances. For example, biotite and plagioclase are reported to limit acid production in waste rock at the Aitik mine in Sweden to the extent that pH values generally remain above about 3.5 even though calcite is absent (Banwart and Malmström, 2001; Linklater et al., 2005;

Strömberg and Banwart, 1994). Rocks at the Samatosum mine in British Columbia are reported to have a high neutralizing capacity in the form of mafic silicates that prevent acid generation (Lawrence and Wang, 1997). Experimental tests also show that mafic silicates can provide an appreciable amount of acid neutralizing capacity that can affect interpretations of standard acid base accounting determinations (Desborough et al., 1998; Jambor et al., 2000; Paktunc, 1999).

The primary objectives of this paper were twofold: First, we wanted to determine if it was feasible to use a geochemical model to represent kinetic processes involved in acid mine drainage based on rate information from the literature and little or no site-specific information other than mineralogy. Second, we wanted to investigate through a series of calculations of rates of silicate mineral dissolution relative to rates of abiotic pyrite oxidation by dissolved O₂ the extent to which standard silicate rock types could potentially provide acid neutralization. Biotic processes involved in pyrite oxidation were not considered because they become important primarily in systems that have already become acidic and consequently have iron concentrations high enough for microbes to thrive through the metabolic processes involved in the oxidation of ferrous ion to ferric ion (Williamson et al., 2006). The purpose of the calculations presented here was to determine if silicates could react fast enough to prevent acid condition from occurring in the first place given a starting of condition of neutral pH. At neutral pH, the abiotic processes are the rate-determining step for pyrite oxidation (Williamson et al., 2006).

A range of generic igneous silicate rock types from silicic to mafic compositions was examined in the calculations to provide a relative measure of their potential to provide neutralization capacity. The effects of secondary mineral formation on solution acidity were also investigated. We focused on dissolved O₂ because it is the primary oxidant for pyrite under neutral pH conditions, whereas ferric ion is more important at pH less than about 4 (Williamson et al., 2005). A near-neutral pH condition is the starting point from which acid generation would either commence or be precluded by silicate dissolution; hence it made sense to consider pyrite oxidation by dissolved O₂ as the initiating process in acidification.

It is recognized by the authors that experimental testing and field observation provide the best determinants of the acid generation potential of any given petrologic system. Thus, the intention of the modeling exercises presented here is not to suggest that they can replace direct observations. Instead, it is our intention to represent the modeling methods as another tool that can be used for rapid and inexpensive assessments of the extent to which different silicate rock types have the potential to mitigate acid rock drainage under a well-defined set of conditions. This type of information can be useful in the preliminary stages of environmental assessment to optimize selection of rock samples for experimental testing and also in the interpretation of observed chemical trends in existing acid rock drainage systems.

Methods

Geochemical model and data sources

The PHREEQC model (Parkhurst and Appelo, 1999, version 2.11) was used for all geochemical calculations with the standard set of thermodynamic data in the default phreeqc.dat datafile. For representing silicate mineral dissolution, a series of rate expressions in the general form developed by Chou and Wollast (1985), Casey and Ludwig (1995) and adopted by Palandri and Kharaka (2004) were added to phreeqc.dat as in:

$$\text{Rate (mole/kg H}_2\text{O/s)} = (A/M)(k_{\text{H}}(\text{H}^+)^a + k_{\text{W}} + k_{\text{OH}}(\text{OH}^-)^b) \quad (6)$$

In Eq. (6), (A/M) is the ratio of mineral surface area to 1 kg H_2O , which is the convention used by PHREEQC, k_H , k_W , and k_{OH} are rate constants for acidic, neutral, and alkaline conditions, and a and b are the dependencies on H^+ and OH^- activities, respectively. Table 1 contains a complete list of the kinetic rate expressions used in calculations.

The rate expressions for the silicates in Table 1 and shown in Fig. 1 are from the extensive compilation of Palandri and Kharaka (2004), who have fit experimental rate data from a wide variety of literature sources to Eq. (6) to provide a data set of silicate dissolution rates that is internally consistent in terms of units, surface areas, and rate law formulation. The rate data considered by Palandri and Kharaka (2004) includes results from both oxic and anoxic experimental conditions. For most silicates, the presence of dissolved oxygen is not a factor for dissolution rate. However, for iron-containing silicates, such as biotite and pyroxenes, dissolved oxygen can increase dissolution rates under acidic pH conditions through surface-catalyzed redox processes (White and Yee, 1985). The magnitude of this effect for the hypothetical starting point of neutral pH conditions used for the calculations here is difficult to quantify. Hence, the rate expressions listed in Table 1 should be considered as broad averages that are appropriate for generalized rate calculations presented here, but may not be necessarily representative of the specific chemical and mineralogical conditions present at any particular site.

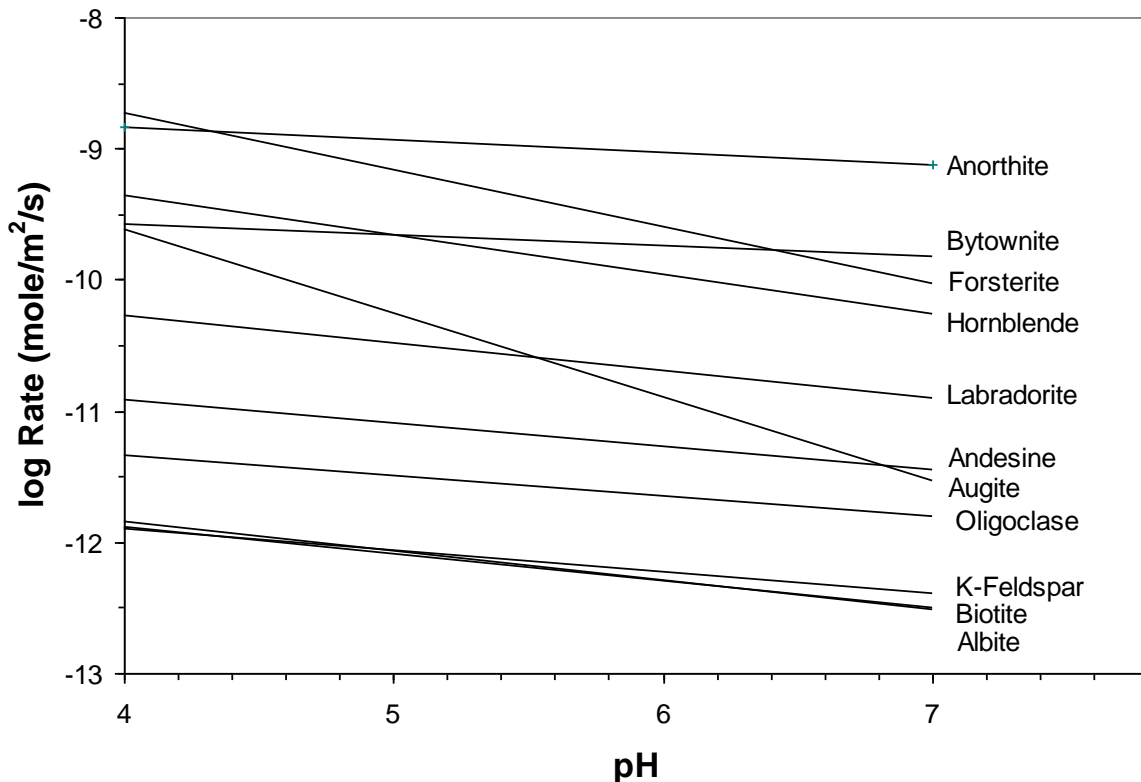


Figure 1. Relative rates of dissolution of silicate minerals using data from the literature compilation of Palandri and Kharaka (2004).

Table 1. List of rate expressions used for calculations from Palandri and Kharaka (2004) (silicates) and Williamson and Rimstidt (1994) (pyrite).

Mineral	Rate Expression	$\log k_H^\dagger$	E_a^*	$\log k_W^\dagger$	E_a^*	$\log k_{OH}^\dagger$	E_a^*
Albite	$k_H(H^+)^{0.457} + k_W + k_{OH}(OH^-)^{0.57}$	-10.16	65	-12.56	69.8	-15.6	71
Oligoclase	$k_H(H^+)^{0.457} + k_W$	-9.67	65	-11.84	69.8	-	-
Andesine	$k_H(H^+)^{0.541} + k_W$	-8.88	53.5	-11.47	57.4	-	-
Labradorite	$k_H(H^+)^{0.626} + k_W$	-7.87	42.1	-10.91	45.2	-	-
Bytownite	$k_H(H^+)^{1.018} + k_W$	-5.85	29.3	-9.82	31.5	-	-
Anorthite	$k_H(H^+)^{1.411} + k_W$	-3.50	16.6	-9.12	17.8	-	-
K-feldspar	$k_H(H^+)^{0.500} + k_W + k_{OH}(OH^-)^{0.82}$	-10.06	51.7	-12.41	38	-21.20	94.1
Biotite	$k_H(H^+)^{0.525} + k_W$	-9.84	22	-12.55	22	-	-
Hornblende	$k_H(H^+)^{0.600} + k_W$	-7.00	75.5	-10.30	94.4	-	-
Augite	$k_H(H^+)^{0.700} + k_W$	-6.82	78	-11.97	78	-	-
Forsterite	$k_H(H^+)^{0.470} + k_W$	-6.85	67.2	-10.64	79	-	-
Pyrite	$k_H(O_2)^{0.500}(H^+)^{-0.11}$	-8.19	-	-	-	-	-

†: mole/m²/s

*: Arrhenius activation energy in kJ/mole.

For pyrite oxidative dissolution, the following generalized rate expression from Williamson and Rimstidt (1994) was used:

$$\text{Rate} = (A/M)k_H(O_2)^{0.5}(H^+)^{-0.11} \quad (7)$$

The rate expression in Eq. (7) is applicable to solutions with pH greater than about 3.5 to 4.0 where pyrite oxidation is dominated by dissolved oxygen rather than ferric ion and the effects of microbial processes, which dominate at lower pH (Williamson et al., 2006). Numerous factors can affect the rate of pyrite oxidation, such as morphology, minor metal substitutions, and crystallinity (Jambor, 1994), and rates in unsaturated conditions (Jerz and Rimstidt, 2004) may be substantially different from the rate described by Eq. (7). The calculations presented in this paper are dependent on Eq. (7), but other rate expressions could also be used to investigate other factors affecting pyrite oxidation that may be specific to a particular site or set of conditions.

Rock Compositions

For the model calculations, a series of seven rock compositions were developed following the general classification of silicic to mafic igneous rocks (Travis, 1955) (Table 2). Standard elemental compositions were used for the individual minerals that comprised the different rock types. For plagioclase, the end-members albite and anorthite were used along with the range of compositions representative of the plagioclase solid solutions.

Solution Conditions

The initial solution composition was based on a standard river water chemistry listed in Langmuir (1997) (Table 3) with the following exceptions. The alkalinity was reduced by 50% to better reflect a poorly buffered drainage system and improve the charge balance. Very low concentrations of Al, Fe, and Si were added to avoid warnings from PHREEQC about basis species being present in equilibrium phases but not in the initial solution composition. In addition, the initial solution had a small deficit in negative charge; hence PHREEQC was allowed to increase the sulfate concentration to achieve a charge-neutral solution.

Table 2. Mineral contents for the seven rock compositions used in model calculations.

Mineral	Qtz						
	Granite	Monz-onite	Monz-onite	Grano-diorite	Qtz Diorite	Diorite	Gabbro
-----Weight Percent-----							
Quartz [SiO ₂]	15	15	5	5	5	0	0
K-feldspar [KAlSi ₃ O ₈]	62	35	30.5	10	5	0	0
Albite [NaAlSi ₃ O ₈]	12.5	10	5	0	0	0	0
Oligoclase [80% Ab+20% An]	0	27.5	45	42.5	28	15	0
Andesine [60% Ab+40% An]	0	0	0	25	39.5	45	0
Labradorite [40% Ab+60% An]	0	0	0	0	0	7.5	45
Bytownite [20% Ab+80% An]	0	0	0	0	0	0	20.5
Anorthite [CaAl ₂ Si ₂ O ₈]	0	0	0	0	0	0	5
Biotite [KMg _{1.5} Fe _{1.5} AlSi ₃ O ₁₀ (OH) ₂]	4	5	5	8	4	2	2
Hornblende [NaCa ₂ Fe ⁺² 4Fe ⁺³ AlSi ₇ O ₂₃ (OH)]	4	5	5	2	5	5	5
Augite [CaMg _{0.5} Fe _{0.5} Si ₂ O ₆]	0	0	2	5	11	18	14
Forsterite [Mg ₂ SiO ₄]	0	0	0	0	0	5	6
Total†	97.5	97.5	97.5	97.5	97.5	97.5	97.5
Pyrite [FeS ₂]	0-3	0-3	0-3	0-3	0-3	0-3	0-3

† Totals were fixed at 97.5% to allow the addition of variable amounts of pyrite.

Table 3. Initial solution composition and equilibrium phases.

Analyte	Concentration (mg/L)	Equilibrium Phases
Ca	15	O ₂ (g) = 0.2 atm
Mg	4.1	CO ₂ (g) = 10 ^{-2.5} atm
K	2.3	Fe(OH) ₃ (a) [†]
Na	6.3	Al(OH) ₃ (a) ^{††}
Cl	7.8	Goethite*
HCO ₃	26	Gibbsite**
SO ₄	3.7	Chalcedony
Al	1.0e-6	Alunite
Fe	1.0e-6	Gypsum
Si	1.0e-6	
pH	7.0	
Temp. (°C)	12	

† Fe(OH)₃(a) + 3 H⁺ = Fe⁺³ + 3 H₂O; log K₂₅ = 4.89

†† Al(OH)₃(a) + 3 H⁺ = Al⁺³ + 3 H₂O; log K₂₅ = 10.80

* FeOOH + 3 H⁺ = Fe⁺³ + 2 H₂O; log K₂₅ = -1.00

** Al(OH)₃ + 3 H⁺ = Al⁺³ + 3 H₂O; log K₂₅ = 8.11

The equilibrium constraints used in the calculations included atmospheric O₂(g) and 10 times atmospheric CO₂(g) (Table 3). The elevated level of CO₂(g) is an estimate of what can be expected for subsurface systems where CO₂(g) generation exceeds the rate at which it can escape. Conditions of equilibrium with common secondary minerals were also specified for the calculations. A set of calculations were conducted for conditions of equilibrium with the solubilities of amorphous Fe and Al hydroxides to represent the initial set of solids that might be expected to form as a result of pyrite oxidation. A second set of calculations was conducted with goethite and gibbsite to represent the solids that would be expected to occur with time and to

provide some information on the sensitivity of the results to the equilibrium phase assemblage. For many of the calculations, conditions of saturation with the solubilities of gypsum, chalcedony, and alunite occurred. When this happened, PHREEQC was used to maintain the solutions at exact saturation with these minerals so that the effects of their equilibria were included in the results (Parkhurst and Appelo, 1999), although they have only a minor effect on pH. Under somewhat more acidic conditions (pH < 4 to 5) than those considered here, schwertmannite or jarosite, and basaluminite, or jurbanite may be more appropriate phases for controlling dissolved iron and aluminum concentrations, but their effects were not examined in the calculations presented here.

Rock-Water System

In a PHREEQC kinetics definition input file, the masses of reactants, such as dissolving minerals, are entered as molar amounts. The default mass of water in a PHREEQC calculation is 1 kg. These two parameters define the default system in terms of moles of minerals per 1 kg of water. Hence, rock-water systems, which contain both solid and water fractions, have to be normalized to this basis with an equation such as:

$$Mineral_{content} \left(\frac{mole}{kg H_2O} \right) = F_{Mineral} \left(\frac{1 - porosity}{porosity} \right) \left(\frac{\rho_{solids}}{\rho_{H_2O}} \right) \left(\frac{1000 g H_2O}{kg H_2O} \right) \left(\frac{mole_{Mineral}}{g_{Mineral}} \right) \quad (8)$$

where $F_{Mineral}$ is the fractional content of the solid portion of the bulk rock comprised of a mineral (g mineral/g solids), porosity is the fluid-filled void fraction of the bulk rock (e.g., 0.35 cm³ H₂O/cm³ rock), ρ_{solids} is the density of the solid portion of the bulk rock (e.g., 2.65 g solids/cm³ solids), ρ_{H_2O} is the density of water (e.g., 1 g H₂O/cm³ H₂O), the 1000 g H₂O/kg H₂O is a conversion factor, and $mole_{Mineral}/g_{Mineral}$ is the molecular weight of the mineral. For example, if a rock contained 1 weight percent pyrite (Py), then the pyrite mineral content for PHREEQC would be:

$$Py_{\frac{mole}{kg H_2O}} = \left(\frac{0.01 g py}{g solids} \right) * \left(\frac{1 - 0.35}{0.35} \right) \left(\frac{2.65 \frac{g}{cm^3}}{1.0 \frac{g}{cm^3}} \right) \left(\frac{1000 g}{kg} \right) \left(\frac{1 mole py}{119.85 g Py} \right) = 0.41 \frac{mole}{kg H_2O} \quad (9)$$

Similar calculations were also conducted to obtain the initial contents of the silicate minerals using the weight percentages listed in Table 1.

The final part of the rock-water system that had to be defined for the calculations was the surface area per kg H₂O or (A/M) term in Eqs. (6) and (7). To obtain surface areas, a number of assumptions were made. First, surface roughness factors that can increase specific surface areas by 0.5 to 1.5 orders of magnitude over geometric values (White, 1995) were ignored. This assumption was made on the basis that only the relative rates of reaction are important for determining effects on solution composition in calculations, whereas surface roughness factors might be expected to affect all rates in approximately the same amount, in effect, canceling each other out. Second, it was assumed that the average size of the silicates was 120 μm. The basis for this assumption is the work of Strömberg and Banwart (1999), who determined that 80% of the reactivity (pyrite oxidation and silicate dissolution) in fresh waste rock occurred in grains with diameter 250 μm or less through studies of water rock interactions at the Aitik mine in Sweden. Hence, we made the assumption that a reasonable average size for the reactive grains was about one half of 250 μm or 120 μm. With these assumptions, the surface areas were

calculated as follows. Silicates other than biotite were assumed to have a cubic shape, which yields a specific surface area (SA) of 0.019 m²/g for a grain size of 120 μm, using the equations for geometric surface area from Hodson (2002),

$$SA \frac{m^2}{g} = \frac{2[(ab) + (bc) + (ac)]}{(abc) * \rho} \quad (10)$$

where a, b, and c are the dimensions of the particles and ρ is the mineral density. Pyrite was also assumed to be cubic shaped with a grain size of 10 μm or about an order of magnitude less than the silicates based on our experience that sulfides are generally finer grained than the host silicates. This assumption results in a specific surface area for pyrite of 0.12 m²/g. Biotite was assumed to be plate-shaped with dimensions of 5x20x40 μm, which yields a specific surface area of 0.213 m²/g (Hodson, 2002). Multiplication of the specific surface area by the mineral contents per kg H₂O gives the surface areas per kg H₂O, which is equal to the (A/M) term in the rate expressions (Eqs. 6 and 7).

The above assumptions on grain size and surface area are important mostly for setting up a system framework to make calculations. We wanted to use values that are reasonably representative of real systems knowing that exact representation of any one system is probably impossible. However, the primary factor that controls the outcome of the calculations is the relative rate at which silicate dissolution and pyrite oxidation take place in response to solution conditions not the selections of grain size and surface area as long as reasonable assumptions are made about the relative difference in sizes of different minerals. In this regard, the selection of a pyrite grain of 10 times less than the silicates is probably the most important assumption. It is beyond the scope of this paper to investigate an effect of the relative grain sizes between different minerals, but it is mentioned here so that its importance is recognized.

To summarize, the system modeled represents a rock or rock matrix that is fully saturated with water. The rock matrix is comprised of individual minerals with an overall composition of different standard igneous rock types and with a single set of grain sizes. The water is maintained at a condition of saturation with atmospheric oxygen and conditions of equilibrium with selected secondary mineral phases are maintained throughout the duration of the calculations. The flow of water through the rock is not simulated, although the system modeled does provide a representation of the chemical evolution of either a stagnant or flowing system for the set of assumptions and reactions included in the calculations.

Results and Discussion

A series of rate calculations were conducted with PHREEQC for each of the rock types listed in Table 2 for a range in pyrite weight percent from 0.05 to 3.0%. It was observed in the calculations that systems that went acidic generally did so within 10 years and systems that did not go acidic remained at a near steady-state pH until the pyrite was eventually consumed. Also, we assumed that a time period of 10 years is a reasonable time frame for the initiation of acid mine drainage if it is going to occur. At 10 years, the calculated pH values were recorded to yield plots of 10-year pH values versus weight percent pyrite in the initial mineral assemblage of each rock type.

Two series of rate calculations were conducted to investigate the effect of selecting amorphous Fe and Al hydroxide secondary solids compared to their more crystalline, less soluble

counterparts of goethite and gibbsite. The selection of secondary Fe and Al solids have been reported have a large effect on model results of oxidation and leaching in pyrite waste rock (Linklater et al., 2005). Thus, one series of rate calculations was conducted for a condition of equilibrium with amorphous ferric hydroxide [$\text{Fe}(\text{OH})_3(\text{a})$, $\log K_{25} = 4.89$] and amorphous aluminum hydroxide [$\text{Al}(\text{OH})_3(\text{a})$, $\log K_{25} = 10.8$]. A second series of calculations was conducted for a condition of equilibrium with goethite [FeOOH , $\log K_{25} = -1.0$] and gibbsite [$\text{Al}(\text{OH})_3$, $\log K_{25} = 8.11$]. In systems with high pyrite contents, other secondary minerals comprised of various aluminum and iron sulfates might also be expected to form if very acidic conditions occur. However, they are not expected to have as much effect on pH as aluminum and ferric oxyhydroxides. Thus, for the purposes of this paper, we have limited the scope to examining the primary effects of aluminum and ferric oxyhydroxides on the results to provide a measure of the range of variability in the results that can be expected.

The results of the calculations for both series of rate calculations were converted into curves that express the 10-year pH as a function of percent pyrite for each rock type (Figs. 2 and 3). The results for both series of calculations show that the 10-year pH decreases significantly as the weight percent pyrite is increased. The major difference between the two series of calculations is that the 10-year pH values for conditions of equilibrium with goethite and gibbsite show a greater decline in pH at lesser amounts of pyrite than the calculations for equilibrium with amorphous Fe and Al hydroxide. This result is expected and is caused by the lower solubilities

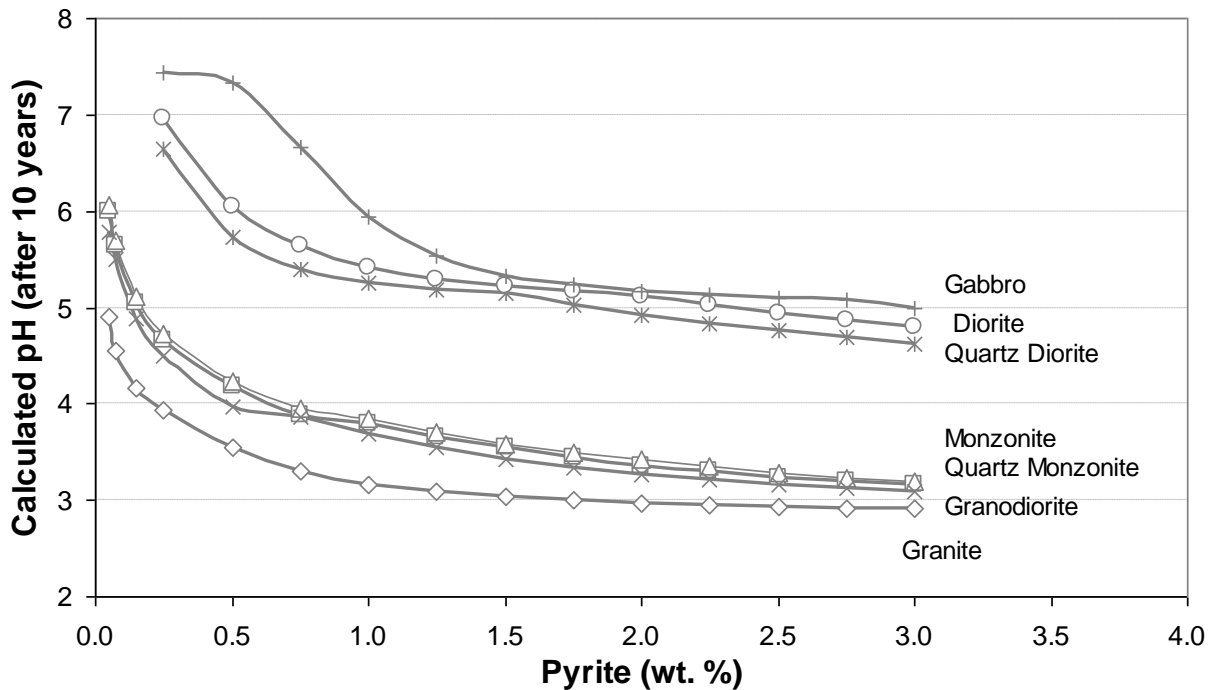


Figure 2. Calculated pH after 10 years in equilibrium with $\text{Fe}(\text{OH})_3(\text{a})$ and $\text{Al}(\text{OH})_3(\text{a})$. (Monzonite and quartz monzonite plot on top of each other.)

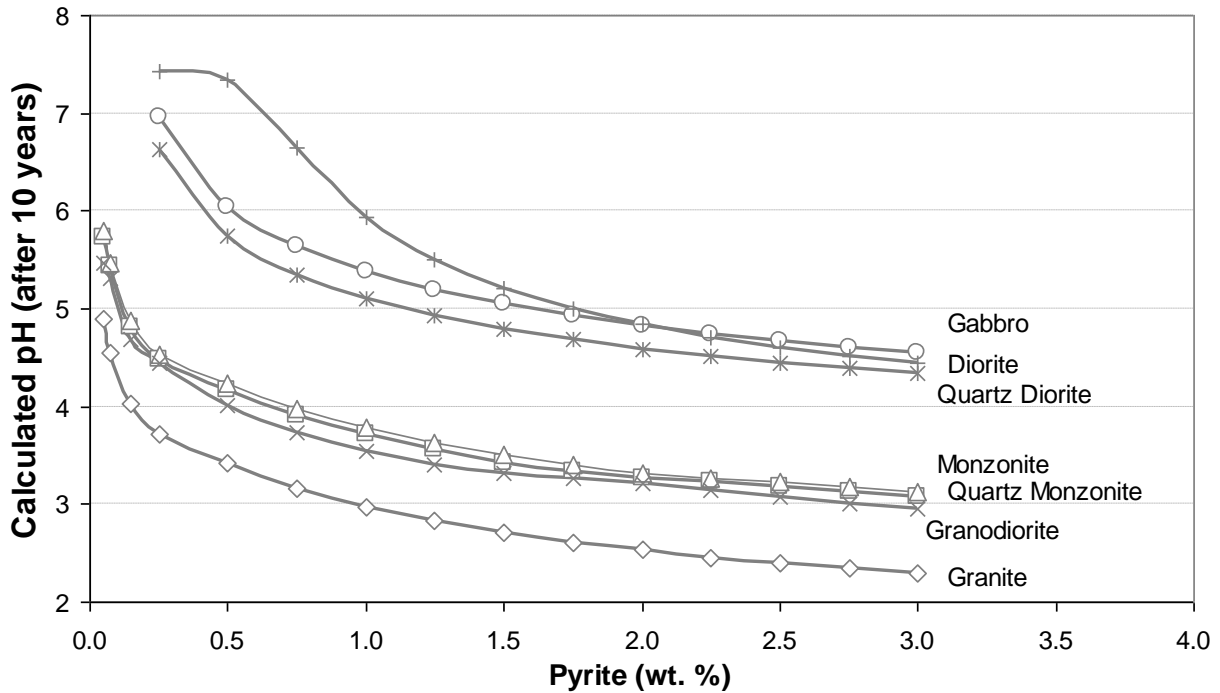


Figure 3. Calculated pH after 10 years in equilibrium with goethite and gibbsite.

of goethite and gibbsite compared to the more soluble amorphous Fe and Al hydroxides. The lower solubilities cause a greater removal of Fe^{+3} and Al^{+3} from solution by reactions such as:



and an associated greater release of acidity, resulting in the lower pH values in the calculations with goethite and gibbsite compared to the amorphous Fe and Al hydroxides.

To obtain an approximation of the amount of acid buffering provided by the different rock types from the calculation results, the curves for each rock type were first examined to determine where they intersected a pH value of 5. The significance of pH = 5 is that it provides a reasonable boundary for discriminating between systems that will become acidic because of pyrite oxidation and systems that will not. In other words, if silicate dissolution is incapable of preventing a decrease in pH from neutral conditions to a value of 5, then it is unlikely to prevent further decline in pH and the system will become an acid rock drainage system. In comparison, if the calculated pH after 10 years remains above 5.0, then the system is unlikely to become acidic over longer periods.

The pyrite percentages at which the 10-year pH values became less than 5.0 in the rate calculations can be converted to acid potential (AP) using the standard formula of:

$$\text{AP} = (\text{Sulfide } \%) (31.25 \text{ kg CaCO}_3/\text{ton rock}) \quad (13)$$

In Eq. (13), the percent sulfide in pyrite is equal to the ratio of sulfide-sulfur to the total molecular weight of pyrite [i.e., Sulfide % = (Pyrite %)(64/119.85)]. Because a 10-year pH

value of 5.0 is used here as convention for discriminating of acidic versus non-acidic conditions, the AP value is equivalent to the neutralization potentials (NP) of the different rock types. The results of these conversions show that the more silicic rock types have very low NP values (Table 4). In comparison, the NP values for the more mafic rock types, such as quartz diorite, diorite, and gabbro, are much higher and indicate that these rock types have the potential to provide significant neutralization potential.

The data in Table 4 also show that the NP values for conditions of equilibrium with goethite and gibbsite are significantly lower than the values calculated for equilibrium with amorphous Fe and Al hydroxides. The large difference in NP values illustrates the importance on modeling outcomes of the selections of secondary solids and indicates that there is range of potential NP values that is characteristic of any given rock-water system that may change over time as a function of the formation of different secondary minerals that are produced as a result of pyrite oxidation and neutralization by silicate mineral dissolution.

Table 4. Calculated total NP values for different rock types.

Rock Type	Equilibrium with Fe(OH) ₃ (a) and Al(OH) ₃ (a)		Equilibrium with Goethite and Gibbsite	
	Pyrite (%)	NP (kg CaCO ₃ /t)	Pyrite (%)	NP (kg CaCO ₃ /t)
Granite	0.02	0.6	0.02	0.6
Quartz Monzonite	0.16	2.7	0.12	2.0
Monzonite	0.18	3.0	0.13	2.2
Granodiorite	0.13	2.2	0.11	1.8
Quartz Diorite	1.75	29.2	1.13	18.9
Diorite	2.41	40.2	1.6	26.7
Gabbro	3.00	50.1	1.75	29.2

Table 5 shows a comparison of the calculated results to experimental results obtained from the literature for a few different rock types. In general, the calculated results are comparable to the experimental results for the silicic rocks for which NP values are very low. However, the calculated NP values are generally much higher than the experimental values for the more mafic rock types. There are a number of potential reasons for the differences between the calculated and experimental results, including relative grain sizes, chemical conditions, times of reactions, mineral compositions, initial solution compositions, etc. In addition, the rate laws used in the calculations are derived from experimental studies of reaction kinetics under conditions far from equilibrium. As systems approach equilibrium, rates can be expected to slow (Lasaga, 1995). This effect is not accounted for in the rate calculations and may be another reason that the calculated NP values are greater than experimental results. While the comparison indicates that the calculated values usually overestimate neutralization capacity for mafic rock types, the calculations do agree in general with the relative changes in neutralization potential that can be expected as a function of mineralogy. The faster dissolving mafic silicates and calcic plagioclase minerals provide substantially more potential to mitigate pyrite oxidation and prevent acid drainage than the silicic rocks in agreement with experimental results (Jambor et al., 2000; White et al., 1999).

Table 5. Comparison of calculated NP values to literature values.

Rock Type	NP Range (kg CaCO ₃ /t) (This study)	NP Range (kg CaCO ₃ /t) (Jambor et al., 2000) [†]	NP Range (kg CaCO ₃ /t) (White et al., 1999)
Granite	0.6	0.9-1.2	
Quartz Monzonite	2.0-2.7	1.1-1.5	
Monzonite	2.2-3.0	1.3-1.9	0.1-2.3 (Latite porphyry)
Granodiorite	1.8-2.2	2.3-2.7	
Quartz Diorite	18.9-29.2	3.1-3.2	
Diorite	26.7-40.2	4.9-5.7	12-24 (Bytownite)*
Gabbro	29.2-50.1	7.3-8.2	0.2-7.4 (Gabbro)

[†] NP values calculated using Sobek- and Lawrence-NP values experimentally determined for individual minerals from Jambor et al. (2000) and weight percents of minerals from Table 2.

* Values for single plagioclase composition equal to bytownite.

Conclusions

The rate calculations show the importance of the mafic mineral content for neutralizing acidity in that minerals, such as calcic plagioclase, forsterite, augite, and hornblende, may react rapidly enough to keep up with the rate of acid generation by pyrite oxidation under the right circumstances. In contrast, felsic minerals, such as K-feldspar and albite, react too slowly to mitigate acid generation. These results are in general agreement with experimental data, although the calculations tend to overestimate neutralization potentials of mafic rock types relative to experimental data. The calculations also show the importance of secondary mineral formation in estimating neutralization potentials. Systems in equilibrium with low solubility secondary solids, such as equilibrium with goethite and gibbsite, yield significantly lower neutralization potentials than system in equilibrium with amorphous Fe and Al hydroxides. Overall, the calculation procedures outlined here show that it is feasible to use geochemical models to estimate neutralization potentials through reaction rate calculations with little information other than estimates of the mineralogical content of the major rock types. These procedures provide an efficient and inexpensive means to conduct scoping studies of likely pH conditions for carbonate-poor rocks that can be used to optimize sample selection for more detailed experimental testing or prediction of potential impacts from acid mine drainage in the absence of detailed experimental data.

Literature Cited

- Banwart, S. A. and M. E. Malmström. 2001. Hydrochemical modeling for preliminary assessment of minewater pollution. *J. Geochem. Expl.* 74, 73-97.
[https://doi.org/10.1016/S0375-6742\(01\)00176-5](https://doi.org/10.1016/S0375-6742(01)00176-5)
- Bigham, J. M., U. Schwertmann, S. J. Traina, R. L. Winland, and M. Wolf. 1996. Schwertmannite and the chemical modeling of iron in acid sulfate waters. *Geochim. Cosmochim. Acta* 60, 2111-2121.
[https://doi.org/10.1016/0016-7037\(96\)00091-9](https://doi.org/10.1016/0016-7037(96)00091-9)
- Casey, W. H. and C. Ludwig. 1995. Silicate mineral dissolution as a ligand exchange reaction. p. 87-117. *In: A. F. White and S. L. Brantley (eds.) Chemical Weathering Rates of Silicate Minerals, Reviews in Mineralogy Vol. 31, Mineral. Soc. Am., Washington, D.C.*

- Chou, L. and R. Wollast. 1985. Steady-state kinetics and dissolution mechanisms of albite. *Am. J. Sci.* 285, 963-993.
<https://doi.org/10.2475/ajs.285.10.963>
- Desborough, G. A., P. H. Briggs, N. Mazza, and R. Driscoll. 1998. Acid-neutralizing potential of minerals in intrusive rocks of the Boulder Batholith in northern Jefferson County, Montana. Open-File Rep. 98-364. U. S. Geol. Surv., Denver, Colorado.
- Goldich, S. S. 1938. A study in rock weathering. *Geology* 46, 17-58.
- Hodson, M. E. 2002. Comments on "Calculations of weathering rate and soil solution chemistry for forest soils in the Norwegian-Russian border area with the PROFILE model" by G. Kopsik, S. Tevedal, D. Aamlid and K. Ven. *Appl. Geochem.* 17, 117-121.
- ICARD. 2000. Proceedings of the Fifth International Conference on Acid Rock Drainage. Soc. for Mining, Metall., Expl., (2 Volumes), Littleton, Colorado.
- Jambor, J. L. 1994. Mineralogy of sulfide-rich tailings and their oxidation products. p. 59-102. In: J. L. Jambor and D. W. Blowes (eds.) *Short Course Handbook on Environmental Geochemistry of Sulfide Mine-Wastes*, Mineral. Assoc. Canada, Vol. 22, Waterloo, Canada, May, 1994.
- Jambor, J. L., J. E. Dutrizac and T. T. Chen. 2000. Contribution of specific minerals to the neutralization potential in static tests. p 551-561. Proceedings 5th International Conference Acid Rock Drainage, Soc. Min. Eng, May 2000.
- Jerz, J. K. and J. D. Rimstidt. 2004. Pyrite oxidation in moist air. *Geochim. Cosmochim. Acta* 68, 701-704.
[https://doi.org/10.1016/S0016-7037\(03\)00499-X](https://doi.org/10.1016/S0016-7037(03)00499-X)
- Langmuir, D. 1997. *Aqueous Environmental Geochemistry*. Prentice-Hall, Upper Saddle River, New Jersey.
- Langmuir, D. and D. O. Whittemore. 1971. Variations in the stability of precipitated ferric oxyhydroxides. P. 209-234. In: R. F. Gould (ed.) *Nonequilibrium Systems in Natural Water Chemistry*. Advances in Chemistry Series 106, Am. Chem. Soc., Washington, D.C.
- Lasaga, A. C. 1995. Fundamental approaches in describing mineral dissolution and precipitation rates. p. 23-86. In: A. F. White and S. L. Brantley (eds.) *Chemical Weathering Rates of Silicate Minerals*, Reviews in Mineralogy Vol. 31, Mineral. Soc. Am., Washington, D.C.
- Lawrence, R. W. and Y. Wang. 1997. Determinations of neutralization potential in the prediction of acid mine drainage. p. 451-464. Fourth Internat. Conf. on Acid Rock Drainage, Proceedings, Vol. II, Vancouver, B.C., May 31-June 6, 1997.
- Linklater, C. M., D. J. Sinclair, and P. L. Brown. 2005. Coupled chemistry and transport modeling of sulphidic waste rock dumps at the Aitik mine site, Sweden. *Appl. Geochem.* 20, 275-293.
<https://doi.org/10.1016/j.apgeochem.2004.08.003>
- MEND. 1997. Proceedings of the Fourth International Conference on Acid Rock Drainage. Vancouver, B.C., May 31-June 6, 1997. Volumes 1-4.
- Millero, F. J. 1985. The effect of ionic interactions on the oxidation of metals in natural waters. *Geochim. Cosmochim. Acta* 49, 547-553.
[https://doi.org/10.1016/0016-7037\(85\)90046-8](https://doi.org/10.1016/0016-7037(85)90046-8)
- Moses, C. O. and J. S. Herman. 1989. Homogeneous oxidation of aqueous ferrous iron at circumneutral pH. *J. Sol. Chem.* 18, 705-725.
<https://doi.org/10.1007/BF00651804>

- Nordstrom, D. K. and C. N. Alpers. 1999. Geochemistry of acid mine waters. Chapt. 6 in *Chemical Weathering Rates of Silicate Minerals*. p. 133-160. *In*: A.F. White and S. L. Brantley (eds.) *Rev. in Mineral. Vol. 31, Mineral. Soc. Am., Washington, D.C.*
- Paktunc, A. D. 1999. Mineralogical constraints on the determination of neutralization potential and prediction of acid mine drainage. *Environ. Geol.* 39, 103-112.
<https://doi.org/10.1007/s002540050440>
- Palandri, J. L. and Y. K. Kharaka. 2004. A compilation of rate parameters of water-mineral interaction kinetic for application to geochemical modeling. *Open-File Rep. 2004-1068, U.S. Geol. Surv., Menlo Park, California.*
- Parkhurst, D.L. and C. A. J. Appelo. 1999. User's guide to PHREEQC (version 2)—A computer program for speciation, Batch-reaction, one-dimensional transport, and inverse geochemical calculations. *Water-Res. Invest. Rep. 99-4259 U.S. Geol. Surv., Denver, Colorado.*
- Strömberg, B. and S. A. Banwart. 1994. Kinetic modeling of geochemical processes at the Aitik mining waste rock site in northern Sweden. *Appl. Geochem.* 9, 583-595.
[https://doi.org/10.1016/0883-2927\(94\)90020-5](https://doi.org/10.1016/0883-2927(94)90020-5)
- Strömberg, B. and S. A. Banwart. 1999. Experimental study of acidity-consuming processes in mining waste rock: some influences of mineralogy and particle size. *Appl. Geochem.* 14, 1-16.
[https://doi.org/10.1016/S0883-2927\(98\)00028-6](https://doi.org/10.1016/S0883-2927(98)00028-6)
- Travis, R. B. 1955. *Classification of Rocks*. Quarterly of the Colorado School of Mines, 50, No. 1 (Reprinted Sept., 1973), Colorado School of Mines, Golden, Colorado.
- White, A. F. 1995. Chemical weathering rates of silicate minerals in soils. Chapt. 9 in *Chemical Weathering Rates of Silicate Minerals*. p. 407-461. *In*: A.F. White and S. L. Brantley (eds.) *Rev. in Mineral. Vol. 31, Mineral. Soc. Am., Washington, D.C.*
- White, A. F. and A. Yee. 1985. Aqueous oxidation-reduction kinetics associated with coupled electron-cation transfer from iron-containing silicates at 25 degrees C. *Geochim. Cosmochim. Acta* 49, 1263-1275.
[https://doi.org/10.1016/0016-7037\(85\)90015-8](https://doi.org/10.1016/0016-7037(85)90015-8)
- White, W. W., K. A. Lapakko, and R. L. Cox. 1999. Static-test methods most commonly used to predict acid-mine drainage: practical guidelines for use and interpretation. p. 325-338. *In*: G. S. Plumlee and M. J. Logsdon (Eds.) *The Environmental Geochemistry of Mineral Deposits, Part A: Processes, Techniques, and Health Issues*. *Reviews in Economic Geology, Vol. 6A, Soc. Econ. Geol., Chelsea, Michigan.*
- Williamson, M. A. and J. D. Rimstidt. 1994. The kinetics and electrochemical rate-determining step of aqueous pyrite oxidation. *Geochim. Cosmochim. Acta* 58, 5443-5454.
[https://doi.org/10.1016/0016-7037\(94\)90241-0](https://doi.org/10.1016/0016-7037(94)90241-0)
- Williamson, M. A., J. D. Rimstidt, and C. S. Kirby 2006, Iron dynamics in acid mine drainage, 7th International Conference on Acid Rock Drainage, 2006 pp 2411-2423